

Experimental study of the momentum correlation of a pseudo-thermal field in the photon counting regime

Giuliano Scarcelli, Alejandra Valencia, and Yanhua Shih

Department of Physics, University of Maryland, Baltimore County, Baltimore, Maryland 21250

Thermal (or pseudo-thermal) radiation has been recently proposed for imaging and interference types of experiments to simulate entangled states. We report an experimental study on the momentum correlation properties of a pseudo-thermal field in the photon counting regime. The characterization and understanding of such a light source in the context of two photon physics, especially its similarities and differences compared to entangled two-photon states, is useful in gaining knowledge of entanglement and may help us to assess the real potential of applications of chaotic light in this context.

The study of thermal radiation has been historically important in optics [1]. Before the invention of the laser, thermal sources were probably the only light sources available in the laboratory for optical experiments and observations. Although coherent light has taken the major role in modern optics laboratory, thermal, or pseudo-thermal, sources are still important for the understanding of fundamental concepts, such as optical coherence and photon statistics [1–4].

Recently it has been theoretically proposed to use thermal, or quasi-thermal, radiation [5] in the context of two-photon imaging and interference [6]. The proposal fits in the lively ongoing discussion about the possibility of using classically correlated light sources to simulate the behavior of entangled photon states. In the past two years, in fact, successful attempts to simulate some of the surprising features of entangled states with classically correlated light have been made [7], leading to an interesting discussion about which features are peculiar to entanglement, and to what extent a classical correlation can simulate them [8]. Furthermore it has been argued that thermal light exhibits exactly the kind of correlations necessary to simulate, at least qualitatively, most of the results obtained in the past through entangled photon states [5].

In this paper we report an experimental study on the momentum correlation properties of thermal radiation in the photon counting regime. A theoretical analysis is also proposed to clarify the physics behind the observed phenomenon, especially the similarities and differences with entangled two-photon states. It may not be quite correct to use the terminology “correlation” to describe the physics behind the experimental observation. In fact, the observed result comes naturally from the *complete absence of correlation*, as is hinted by the same name of chaotic light.

In principle the term “thermal radiation” should refer

only to radiation coming from a blackbody in thermal equilibrium at some temperature T . But in reality, some characteristics of true thermal fields, like the extreme shortness of their coherence time, have imposed serious obstacles to their use in actual experiments, and therefore since the early days of quantum optics there has been a great interest in the realization of more utilizable sources that could simulate the behavior of true thermal fields (gas discharge lamps, randomized lasers etc.). We usually describe these kind of sources as pseudo-thermal; they are actually all chaotic light sources that can be modelled as a collection of independent atoms emitting radiation randomly [9]. The most commonly used among the pseudo-thermal fields is the one developed by Martienssen and Spiller [10] in the mid of 1960 's. The principle of the generation is very simple: coherent laser radiation is focused on a rotating ground glass disk so the scattered radiation is chaotic with a Gaussian spectrum.

We start by describing the light source used in this experiment. We experimentally studied the characteristics of the source to be sure that it indeed behaved like a thermal field. To this purpose we used an experimental setup similar to the one that was later used to perform the momentum correlation measurement (Fig. 1). First we focused on the temporal behavior and repeated a historical experiment of Arecchi et al [11]. The point of the experiment was to study the time distribution of the coincidence counts coming from the source under study. Fig. 2 shows the results of the measurements. Basically we plot a histogram of the number of coincidence counts versus the time difference of the photon registration clicks from the two detectors. The temporal behavior of our source is similar to the one obtained with light coming from stars and gas discharge lamps [12–14], but with a higher coherence time (around $1\mu s$, mainly determined by the rotation speed of the disk and the properties of the grit of the ground glass). In practice this graph is also useful for “calibrating” the coincidence time window; in fact in the rest of the experiment we set a window of about 600 ns around the peak of Fig. 2 and measured the number of coincidence counts in that window. Then we studied the spatial behavior of the coincidence counts using the setup in Fig. 1. The point of this measurement is to study the behavior of the spatial correlations when the size of the source is varied. This kind of measurement is basically the one used to determine the angular size of the stars in Hanbury-Brown and Twiss stellar interferometry. Experimentally we fixed detector D_1 in one position and scanned horizontally the position of detector D_2 for different sizes of the source obtained by focusing

or defocusing the He-Ne laser onto the rotating disk. The results are shown in Fig. 3. As expected, the bigger is the angular size of the source, the smaller is the width of the correlation function, in agreement with stellar interferometric predictions.

These two measurements confirmed that our source simulated both spatially and temporally the behavior of thermal radiation. We then proceeded on measuring the momentum-momentum correlation of the field. The setup for the measurement is shown in Fig. 1. After the source, a lens (L) of focal length $f = 75\text{cm}$ was inserted, and then the radiation was split by a non-polarizing cube beam splitter ($l = 25\text{mm}$). In the focal plane of the lens L we put the detection system composed of two horizontally displaceable fibers ($60\mu\text{m}$ diameter) connected to two single-photon counting modules. The output pulses from the two detectors were then sent to an electronic coincidence circuit. The setup is designed to study the momentum properties of the fields, in fact the lens L was close to the source and the detectors were placed in its focal plane to ensure the far-field condition. In this situation, in principle, the fiber tip (detector) scans the transverse wavevector plane, or transverse momentum plane, of the field. Therefore by scanning the fibers in the horizontal direction continuous information about the behavior of each k-vector (momentum) of the field will be obtained.

We performed three sets of measurements for three different position of detector D_1 ; in every measurement we kept the position of D_1 fixed and scanned horizontally the position of detector D_2 . The results are shown in Fig. 4. It is clear that the correlation function “followed” the movement of detector D_1 ; a shift in the position of D_1 , causes a shift in the same direction of the correlation function. The natural deduction from this measurement is that the field is indeed correlated in momentum: in fact every time a position of D_1 is fixed, one k-vector from the source is selected, therefore the behavior of the coincidence counts show that only one k-vector arriving at D_2 is correlated to the selected k-vector arriving at D_1 . In the central part of Fig. 4 the single counts are reported, notice that (1) the single counts are flat over the entire range of detection suggesting the completely random transverse distribution of the field; (2) the low level of photon counts (60000 per second) suggests that we were effectively operating in the condition of only two photons present in the time duration of interest.

The phenomenological conclusion of these measurements would then be that the pseudo-thermal field we have measured is indeed correlated in momentum. This is a property that makes this source particularly interesting to study in comparison with entangled photon pairs produced in Spontaneous Parametric Down Conversion (SPDC) in the context of two-photon imaging and interference features [6,5]. However, the predicted, and now experimentally measured, analogy between the effects obtained with entangled photons and thermal radiation has to be analyzed very carefully. In order to clarify the point

let us justify theoretically the measured experimental effect. The quantity that rules the experiments involving coincidence measurements is the second-order Glauber correlation function [15]:

$$G^{(2)}(t_1, \mathbf{x}_1; t_2, \mathbf{x}_2) \equiv \text{Tr}[\hat{\rho} E_1^{(-)}(t_1, \mathbf{x}_1) E_2^{(-)}(t_2, \mathbf{x}_2) E_2^{(+)}(t_2, \mathbf{x}_2) E_1^{(+)}(t_1, \mathbf{x}_1)]. \quad (1)$$

Where \mathbf{x}_i is a vector in the plane of the i^{th} detector perpendicular to the direction of propagation of the radiation, $\hat{\rho}$ represents the density matrix of the quantum state under consideration, and $E_i^{(\pm)}(t_i, \mathbf{x}_i)$, $i = 1, 2$, are positive-frequency and negative-frequency components of the field at detectors D_1 and D_2 that can be written as:

$$E_i^{(+)}(t_i, \mathbf{x}_i) = \sum_{\mathbf{k}} \sqrt{\frac{\hbar\omega}{2\epsilon_0 V}} g_i(\mathbf{x}_i, \mathbf{k}) a_{\mathbf{k}} e^{-i\omega t_i}. \quad (2)$$

Here $g_i(\mathbf{x}_i, \mathbf{k})$ stands for the Green's function associated with the propagation of the field towards the i^{th} detector [16]. Plugging the expression of the electric fields in Eq. 1, we obtain the equal time second-order Glauber correlation function in the following form:

$$G^{(2)}(\mathbf{x}_1; \mathbf{x}_2) \propto \sum_{\mathbf{k}} \sum_{\mathbf{k}'} \sum_{\mathbf{k}''} \sum_{\mathbf{k}'''} g_1^*(\mathbf{x}_1, \mathbf{k}) g_2^*(\mathbf{x}_2, \mathbf{k}') \times g_2(\mathbf{x}_2, \mathbf{k}'') g_1(\mathbf{x}_1, \mathbf{k}''') \text{Tr}[\hat{\rho} a_{\mathbf{k}}^\dagger a_{\mathbf{k}'}^\dagger a_{\mathbf{k}''} a_{\mathbf{k}'''}]$$

Let us examine the last term of Eq. 3, in particular the density matrix of the state of the radiation we are studying. Usually the density matrix that is used for single mode thermal light is expressed in the number state basis as follows [9] [17]:

$$\hat{\rho} = \sum_n \frac{\langle n \rangle^n}{(1 + \langle n \rangle)^{1+n}} |n\rangle \langle n| \quad (4)$$

In the multimode case we can take $\{|n_{\mathbf{k}}\rangle\}$ as basis vectors, where the symbol $\{n_{\mathbf{k}}\}$ indicates a set of number of photons $n_{\mathbf{k}_1}, n_{\mathbf{k}_2}, n_{\mathbf{k}_3}$ etc. in the modes $\mathbf{k}_1, \mathbf{k}_2, \mathbf{k}_3$ respectively, and $\{|n_{\mathbf{k}}\rangle\}$ are product states of the number states $|n_{\mathbf{k}}\rangle$ of each mode \mathbf{k} . In thermal and chaotic light the different modes of the field are independent [9], thus the total density matrix will be the product of the contributions from the different modes as follows:

$$\hat{\rho} = \sum_{\{n_{\mathbf{k}}\}} |\{n_{\mathbf{k}}\}\rangle \langle \{n_{\mathbf{k}}\}| \prod_{\mathbf{k}} \frac{\langle n_{\mathbf{k}} \rangle^{n_{\mathbf{k}}}}{(1 + \langle n_{\mathbf{k}} \rangle)^{1+n_{\mathbf{k}}}} \quad (5)$$

where $\langle n_{\mathbf{k}} \rangle$ represent the average number of photons in mode \mathbf{k} .

A comparison between the density matrix that describes the thermal radiation and the state of the entangled photons from SPDC can readily clarify the intrinsic

difference between the two sources. While in the thermal case it is intuitive and apparent from Eq. 5 that the different modes of the radiation are completely independent, it is immediately clear from the state of the SPDC radiation that there is perfect correlation in momentum exhibited by the source.

The trace in Eq. 3 turns out to be:

$$\text{Tr}[\hat{\rho}a_{\mathbf{k}}^\dagger a_{\mathbf{k}'}^\dagger a_{\mathbf{k}''} a_{\mathbf{k}'''}] = \langle n \rangle^2 (\delta_{\mathbf{k},\mathbf{k}''} \delta_{\mathbf{k}',\mathbf{k}'''} + \delta_{\mathbf{k},\mathbf{k}'''} \delta_{\mathbf{k}',\mathbf{k}''}) \quad (6)$$

where we have assumed the average number of photons in each mode to be constant (as is confirmed by the single counts behavior in Fig. 4). Plugging the previous result in Eq. 3 we obtain the following expression for the second-order correlation function:

$$G^{(2)}(\mathbf{x}_1; \mathbf{x}_2) \propto \int d^2 \mathbf{q} |g_1(\mathbf{x}_1, \mathbf{q})|^2 \int d^2 \mathbf{q} |g_2(\mathbf{x}_2, \mathbf{q})|^2 + \left| \int d^2 \mathbf{q} g_1^*(\mathbf{x}_1, \mathbf{q}) g_2(\mathbf{x}_2, \mathbf{q}) \right|^2. \quad (7)$$

Where \mathbf{q} is the transverse component of the k-vector. Notice that we have converted the summation of Eq. 2 into an integral. It is easy to see that $\int d^2 \mathbf{q} |g_i(\mathbf{x}_i, \mathbf{q})|^2$ will actually lead to the number of single counts n_i of the i^{th} detector. The expression can be further simplified:

$$G^{(2)}(\mathbf{x}_1; \mathbf{x}_2) \propto 1 + \frac{\left| \int d^2 \mathbf{q} g_1^*(\mathbf{x}_1, \mathbf{q}) g_2(\mathbf{x}_2, \mathbf{q}) \right|^2}{n_1 n_2} \quad (8)$$

Inserting the Green's functions associated to the optical setup into Eq. 8 we obtain:

$$G^{(2)}(\mathbf{x}_1; \mathbf{x}_2) \propto 1 + \left[\frac{J_1(\pi a |\mathbf{x}_1 - \mathbf{x}_2| / \lambda f)}{\pi a |\mathbf{x}_1 - \mathbf{x}_2| / 2 \lambda f} \right]^2 \quad (9)$$

where J_1 is the Bessel function of the first order and a is the size of the source. This result explains clearly the experimental observations of both Fig. 3 and Fig. 4. In fact, it predicts that the bigger the size of the source, the smaller is the width of the correlation, and above all it predicts that shifting the position of detector D_1 will cause the observed shift of the correlation function. Notice that, due to the first term in Eq. 9, the maximum achievable visibility in these kind of experiments is 33%.

Although the theoretical calculations are able to predict the experimental observations, the physical interpretation of the experimental results and mathematical formalism remains yet to be fully explained and understood. To clarify this point, let us focus for a moment on the following quantities:

$$\begin{aligned} \langle a_{\mathbf{k}}^\dagger a_{\mathbf{k}'} \rangle &\equiv \text{Tr}[\hat{\rho} a_{\mathbf{k}}^\dagger a_{\mathbf{k}'}] \\ \langle a_{\mathbf{k}}^\dagger a_{\mathbf{k}'} a_{\mathbf{k}''} a_{\mathbf{k}'''} \rangle &\equiv \text{Tr}[\hat{\rho} a_{\mathbf{k}}^\dagger a_{\mathbf{k}'} a_{\mathbf{k}''} a_{\mathbf{k}'''}] \end{aligned} \quad (10)$$

Substituting into this equation the expression for the density matrix that describes our source we obtain:

$$\langle a_{\mathbf{k}}^\dagger a_{\mathbf{k}'} \rangle = \langle n \rangle \delta_{\mathbf{k},\mathbf{k}'} \quad (11)$$

$$\langle a_{\mathbf{k}}^\dagger a_{\mathbf{k}'}^\dagger a_{\mathbf{k}''} a_{\mathbf{k}'''} \rangle = \langle n \rangle^2 (\delta_{\mathbf{k},\mathbf{k}''} \delta_{\mathbf{k}',\mathbf{k}'''} + \delta_{\mathbf{k},\mathbf{k}'''} \delta_{\mathbf{k}',\mathbf{k}''}) \quad (12)$$

Notice that relations of the kind in Eq. 11 are generally used in statistics to express the absolute *statistical independence* of the variates under study. In this case therefore Eq. 11 can be interpreted as the mathematical expression of the *lack of correlation* between different modes of the field [1] and the experimental observations would be a natural manifestation of this property.

As far as Eq. 12 is concerned, in the context of entangled photon states, a formally similar equation is usually considered explicative of the perfect momentum correlation between the two entangled photons due to the phase matching conditions of the nonlinear process inside the crystal. The interpretation of this mathematical relation in terms of correlation between k-vectors could be misleading in the case of chaotic light. In fact, it would employ a terminology peculiar to entangled photons for a process that is intrinsically different.

Besides the physical interpretation, however, the theoretical and experimental results reveal that the source under study, and thus thermal radiation in general, is promising for two-photon interference type experiments, except for the lower visibility (33% maximum) [18]. From a fundamental point of view it can represent a perfect tool for studying the differences and/or the analogies between quantum entanglement and its classical simulation.

In conclusion, we have experimentally studied the far-field momentum ‘‘correlation’’ of chaotic light fields and we have provided a theoretical explanation of the results with a physical interpretation of the phenomenon. The observed correlation is in fact the experimental evidence of the complete *absence of correlation* between different modes of the radiation. The experiment can help us to assess to what extent thermal or pseudo-thermal fields might be employed to simulate certain features of entangled photons in the context of two-photon imaging and interference.

-
- [1] L.Mandel and E.Wolf, *Optical coherence and quantum optics* (Cambridge University Press,1995).
 - [2] R. Hanbury-Brown and R.Q. Twiss, *Nature* **177**, 28 (1956); 178, 1046, 1447 (1956).
 - [3] U. Fano, *Am. J. Phys.* **29**, 539 (1961).
 - [4] R.J. Glauber, *Phys. Rev.* **131**, 2766 (1963).
 - [5] A.Gatti, E. Brambilla, M.Bache and L.A. Lugiato, *Phys. Rev. A* **70**, 013802, (2004); K.Wang and D. Cao, *quant-ph/0404078*.
 - [6] T.B. Pittman, Y.H. Shih, D.V. Strekalov, and A.V. Sergienko, *Phys. Rev. A* **52**, R3429 (1995); D.V.

- Strekalov, A.V. Sergienko, D.N. Klyshko, and Y.H. Shih, Phys. Rev. Lett. **74**, 3600 (1995).
- [7] R.S. Bennink, S.J. Bentley and R.W. Boyd, Phys. Rev. Lett **89**, 113601 (2002).
- [8] A.F. Abouraddy, B.E.A. Saleh, A.V. Sergienko and M.C. Teich, Phys. Rev. Lett. **87**, 123602 (2001); A. Gatti, E.Brambilla and L.A. Lugiato, Phys. Rev. Lett., **90**, 133603 (2003); M.H. Rubin, quant-ph/0303188; M.D'Angelo, Y.H. Kim, S.P. Kulik and Y. Shih, Phys. Rev. Lett. **92**, 233601 (2004).
- [9] R. Loudon, *The quantum theory of light* (2nd edition, Oxford University Press,1983).
- [10] W. Martienssen and E. Spiller, Am. J. Phys. **32**, 919 (1964).
- [11] F.T. Arecchi, E. Gatti, and A. Sona, Phys. Lett. **20** 27 (1966).
- [12] R. Hanbury-Brown, *Intensity Interferometer* (Taylor and Francis Ltd, London 1974).
- [13] D.B. Scarl, Phys. Rev. Lett. **17** 663 (1966).
- [14] D.T. Phillips, H. Kleinman, and S.P. Davis, Phys. Rev. **153** 113 (1967).
- [15] R.J. Glauber, Phys. Rev. **130**, 2529 (1963) ; U.M. Titulaer and R.J. Glauber, Phys. Rev. **140**, B676 (1965).
- [16] M.H. Rubin, Phys. Rev. A **54**, 5349, (1996)
- [17] M.O. Scully and M.S. Zubairy, *Quantum Optics* (Cambridge University Press, 1997).
- [18] D.N. Klyshko, Phys. Lett. A **163**, 349, (1992)

FIG. 1. Sketch of the experimental setup

FIG. 2. Histogram of number of joint detection counts vs time difference of the two photo-electron events. The size of each channel is 0.3 ns.

FIG. 3. Normalized second order correlation function vs position of detector D_2 . The various sets of data (points) are for different sizes of the pseudo-thermal source (circles $\sim 150\mu\text{m}$; squares $\sim 350\mu\text{m}$; triangles $\sim 550\mu\text{m}$; diamonds $\sim 1100\mu\text{m}$) and agree with the theoretical expectation (solid lines).

FIG. 4. Normalized second order correlation function vs position of detector D_2 for three fixed positions of detector D_1 : (a) $x_1 \simeq -1.75\text{mm}$; (b) $x_1 \simeq 0\text{mm}$; (c) $x_1 \simeq 1.75\text{mm}$ (source size $\sim 550\mu\text{m}$). In part (b) is shown also a plot of single counts vs position of the detector for both D_1 (filled squares) and D_2 (hollow squares). The level of the counts is around 60000 per second.

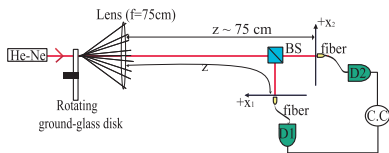


Figure 1. Giuliano Scarcelli, Alejandra Valencia, and Yanhua Shih.

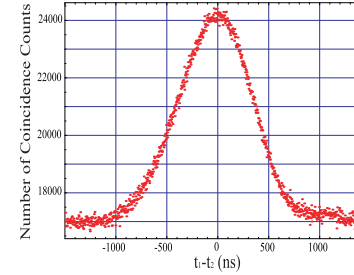


Figure 2. Giuliano Scarcelli, Alejandra Valencia, and Yanhua Shih.

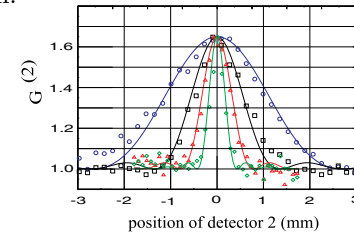


Figure 3. Giuliano Scarcelli, Alejandra Valencia, and Yanhua Shih.

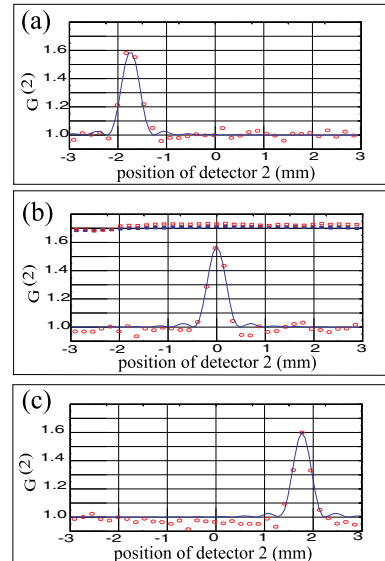


Figure 4. Giuliano Scarcelli, Alejandra Valencia, and Yanhua Shih.